Direct observation of magnetic phase coexistence and magnetization reversal in a Gd0.67Ca0.33MnO3 thin film

Jeehoon Kim, N. Haberkorn, Leonardo Civale, Evgeny Nazaretski, Paul Dowden et al.

Related Articles

Spin configurations in Co2FeAl0.4Si0.6 Heusler alloy thin film elements
Appl. Phys. Lett. 99, 182510 (2011)

Quantum tunneling of the Bloch point in a magnetic film with strong uniaxial magnetic anisotropy
Low Temp. Phys. 37, 690 (2011)

Evolution of magnetic bubble domains in manganite films
Appl. Phys. Lett. 99, 042503 (2011)

360° domain wall mediated reversal in rhombic Co/Cu/NiFe magnetic rings
Appl. Phys. Lett. 98, 252506 (2011)

Phase-field simulation of electric-field-induced in-plane magnetic domain switching in magnetic/ferroelectric layered heterostructures
J. Appl. Phys. 109, 123917 (2011)

Additional information on Appl. Phys. Lett.

Journal Homepage: http://apl.aip.org/

Journal Information: http://apl.aip.org/about/about_the_journal

Top downloads: http://apl.aip.org/features/most_downloaded

Information for Authors: http://apl.aip.org/authors

Direct observation of magnetic phase coexistence and magnetization reversal in a $Gd_{0.67}Ca_{0.33}MnO_3$ thin film

Jeehoon Kim,[1,a)] N. Haberkorn,[1] Leonardo Civale,[1] Evgeny Nazaretski,[2] Paul Dowden,[1] Avadh Saxena,[1] J. D. Thompson,[1] and Roman Movshovich[1]

[1]Los Alamos National Laboratory, Los Alamos, New Mexico 87545, USA
[2]Brookhaven National Laboratory, Upton, New York 11973, USA

We have investigated the ferrimagnetic domain structure in a $Gd_{0.67}Ca_{0.33}MnO_3$ thin film using magnetic force microscopy. We observe clear signs of phase separation, with magnetic islands embedded in a non-magnetic matrix. We also directly visualize the reversal of magnetization of ferrimagnetic domains as a function of temperature and attribute it to a change in the balance of magnetization of anti-aligned Mn and Gd sublattices. © 2012 American Institute of Physics. [doi:10.1063/1.3676045]

Mixed-valent perovskite manganites $A_{1-x}B_xMnO_3$ (A and B are rare-earth and divalent alkaline elements, respectively), such as La-based manganites, have been studied extensively in recent years.[1–4] These materials exhibit a colossal magnetoresistance (CMR) effect for a wide range of dopings centered at $x = 1/3$ where the double exchange mechanism is maximized.[5] The resulting combination of fascinating physical phenomena and a potential for technological applications have been the driving force in sustaining high interest in these compounds.[1–4] Electronic inhomogeneity and phase separation are ubiquitous in doped manganites, and the resulting CMR effect is driven by percolative transport.[6] CMR manifests itself by a dramatic drop in resistivity and a discontinuous decrease in the equilibrium Mn-O bond length at a first order phase transition in an applied magnetic field.[7,8] Their complex electronic structure and a variety of competing interactions lead to a rich ensemble of ground states in this family of compounds.

In this letter, we report a low temperature magnetic force microscopy (MFM) investigation of $Gd_{0.67}Ca_{0.33}MnO_3$ (GCMO), a compound with an insulating ferrimagnetic (FIM) ground state. Compared to other ferromagnetic (FM) perovskite manganites, GCMO exhibits a relatively low Curie temperature (T_C), and its small structural tolerance factor $t < 0.89$ (Refs. 9 and 10) leads to a robust insulating ground state. Magnetic properties of the system reflect those of the two sublattices of Mn and Gd ions (see below). The different temperature dependence of magnetization of each of the two sublattices results in a change of sign of the total magnetization as a function of temperature at a characteristic compensation temperature T_{comp}, where the Mn and Gd sublattices have magnetic moments of the same magnitude and opposite direction.[9–11] A small tolerance factor, a structural distortion, and the antiferromagnetic interaction between Gd and Mn sublattices yield remarkable properties, such as a giant magnetostrictive effect in a wide temperature range[12] and inhomogeneous FIM-like behavior with an exchange bias effect close to T_{comp}.[13] Low values of the saturation magnetization (M_S) suggest phase coexistence.[12,13] MFM studies described below, with the wide range of field and temperature

employed, allow us to visualize the magnetic structure of GCMO and provide direct evidence of phase separation. The magnetization reversal at T_{comp} of *each individual* domain provides strong support for the scenario of anti-aligned Mn and Gd sublattices with the Gd (Mn) magnetization dominating below (above) T_{comp}.

The $Gd_{0.67}Ca_{0.33}MnO_3$ thin film was grown by pulsed-laser deposition (PLD) on a $SrTiO_3$ (100) substrate from a commercial target with the same chemical composition. The substrate temperature was kept at $790\,°C$ in an oxygen atmosphere at a pressure of $200\,mTorr$. After deposition, the O_2 pressure was increased to $200\,Torr$, and the temperature was decreased to room temperature at a rate of $30\,°C/min$. Bulk GCMO is an orthorhombic perovskite (Pbnm (No. 62); $a = 5.52\,Å$, $b = 5.34\,Å$, $c = 7.50\,Å$).[13,14] The GCMO film was examined by x-ray diffractometry and was found to be single phase with a (00l) orientation. The lattice parameters ($a = 5.55(2)\,Å$, $b = 5.36(2)\,Å$, and $c = 7.50(1)\,Å$) were determined using (00l), (200), and (020) reflections from a four-circle diffractometer/goniometer. No additional peaks due to secondary phases or different crystalline orientations were observed. The rocking curve width around the (004) peak of the film was ~0.27°. The film thickness of $45\,nm$ was determined by a low-angle x-ray reflectivity measurement with an angular resolution of 0.005°.

A quantum design superconducting quantum interference device (SQUID) magnetometer was used for measurements of the global magnetization with the magnetic field oriented perpendicular to the film surface. All localized MFM measurements described in this letter were performed in a home-built low-temperature MFM apparatus.[15] MFM images were taken in a frequency-modulated mode, with the tip-lift height of $100\,nm$ above the sample surface. High resolution SSS-QMFMR cantilevers,[16] magnetized along the tip axis in a field of $3\,T$, were used for MFM measurements; the external magnetic field was always applied perpendicular to the film surface and parallel to the MFM tip.

Fig. 1(a) shows the field-cooled (FC) magnetization M as a function of temperature at different values of applied magnetic field H. The temperature dependence of magnetization was discussed previously by Snyder *et al.*[10] GCMO undergoes a phase transition from a paramagnetic insulating
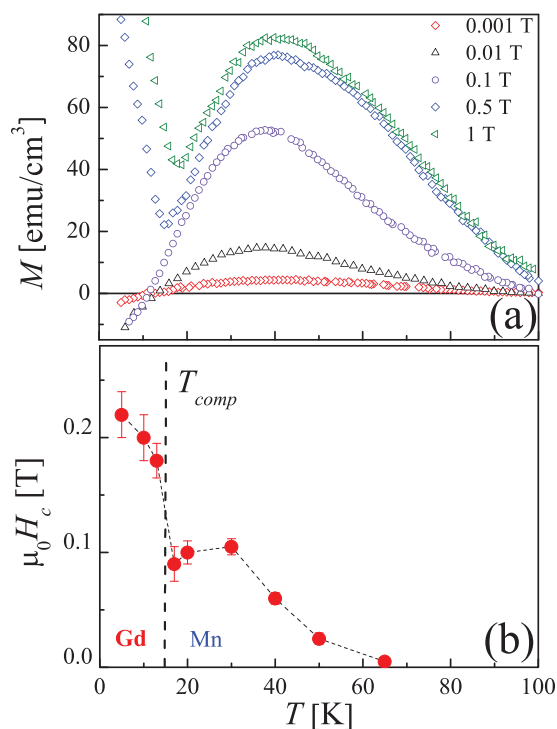
a)Electronic mail: jeehoon@lanl.gov.

FIG. 1. (Color online) (a) Field-cooled $M(T)$ curves in different magnetic fields (H). (b) Coercive field (H_c) as a function of temperature obtained from magnetic hysteresis loops.

to a ferromagnetic insulating state, associated with the ferromagnetic ordering of Mn cations, at $T_C \approx 80$ K. The local field due to FM order in the Mn sublattice and the negative f-d exchange interaction on the Gd spins force the moments on the Gd sublattice to be anti-aligned to those in the Mn sublattice. The Mn sublattice dominates the magnetization at high temperature, but the absolute magnitude of magnetization of the Gd sublattice grows faster when the temperature is reduced. Consequently, the total magnetization M reaches a maximum value close to 50 K (see Fig. 1), starts to decrease with decreasing temperature, and goes toward zero at $T_{comp} \approx 15$ K in low fields (T_{comp} depends on H), where magnetizations of the Mn and Gd sublattices compensate each other. Below T_{comp} the local magnetization of Gd is larger than that of Mn, $|M_{Gd}| > |M_{Mn}|$, and the sign of the total magnetization is determined by the direction of magnetization of the Gd sublattice. When the applied magnetic field H is below the coercive field H_c of the system at T_{comp}, the magnetization of the Gd sublattice is locked in a direction opposite to the applied field, and the total magnetization is negative below T_{comp}. For $H > H_c$ the magnetization is reversed immediately below T_{comp}, producing a characteristic sharp kink and a V-shape in the data. This sharp reversal of the change in magnetization (from decreasing to increasing with decreasing temperature) is facilitated by a strong decrease of H_c at T_{comp}, as shown in Fig. 1(b), which is determined on the basis of an analysis of full hysteresis curves at different temperatures (data not shown). The positive offset of M at the kink at 0.5 and 1 T in Fig. 1(a) is due to a paramagnetic background. All magnetic transition temperatures observed in the film are in good agreement with the values previously reported for bulk polycrystal and single crystal samples.[10,13,14] The data at 0.1 T has a clear kink as it crosses

$M = 0$ and T_{comp}, indicating that some small number of the magnetic domains flip their orientation at T_{comp}. This is consistent with the bulk measurements of $H_c \approx 0.1$ T at T_{comp}, and points to coercive field in this system being a local property, probably dependent on the magnetic domain's size, shape, and environment.

The MFM images depicted in Figs. 2(a)–2(c) were taken sequentially at 4 K ($T < T_{comp}$), 10 K ($T \approx T_{comp}$), and 15 K ($T > T_{comp}$), respectively, in a magnetic field of 1 mT (below H_c) applied above T_C (field-cooled data). The dashed circles in Figs. 2(a)–2(c) show the same sample region (thermal drifts are negligible for images taken below 15 K, see below). Regions of a non-zero magnetic signal, either blue or red, change color as the temperature changes from 4 to 15 K, but the green areas remain green in all images [(a)-(c)] in Fig. 2. The sample, therefore, is phase separated into FIM (blue and red) and non-magnetic (green) regions.[17] At 4 K (Fig. 2(a)) Gd dominates the magnetization of FIM domains, as depicted schematically in Fig. 2(e). Red islands in Fig. 2(a), therefore, represent those parts of the sample where Gd magnetic moments point "down," and the blue regions are those with Gd magnetic moments pointing "up." At 15 K (Fig. 2(c)) all of the red regions switch to blue, signaling a reversal in their magnetization, as Mn magnetization is dominant above $T_{comp} \approx 12$ K. This situation is depicted schematically in Fig. 2(f). The small magnetic contrast across the sample at 10 K (see Fig. 2(b)) indicates almost equal magnetic contributions of the anti-aligned Gd and Mn sublattices in FIM regions near T_{comp}. In addition, Fig. 2(b) demonstrates the domains' breakup and a reduction in their size close to T_{comp} (at 10 K). This phenomenon is consistent with the exchange bias effect previously observed in single crystals.[13] The reduction of the size of FIM domains close to T_{comp} also leads to a decrease of the coercive field (see Fig. 1(b)).[14,18]

Fig. 2(d) shows a cross-correlation map between images (a) and (c) and allows us to investigate qualitatively the temperature evolution of magnetic domains in the sample. The large negative value in the center of the cross-correlation map demonstrates the anti-correlation between 4 and 15 K magnetization data in Fig. 1(a), indicating that red and blue islands reverse their magnetization (and colors) upon the temperature change from 4 to 15 K. The central location of the cross-correlation minimum also demonstrates the small thermal drift in our MFM apparatus.

Figs. 3(a)–3(d) show MFM images obtained at 4 K after field-cooling the GCMO sample through T_C in 0, 0.1, 0.5, and 1 T applied fields. In order to understand the thermal and field evolution of the sample's magnetization we evaluated cross-correlation maps for these images. No correlation was observed between data sets obtained at 0 and 0.1 T (panels (a) and (b)) as shown in Fig. 3(e) and 0.1 and 0.5 T (panels (b) and (c)) as shown in Fig. 3(f). The lack of cross-correlation indicates significant evolution of the spin magnetization due to the reversal process inside FIM clusters in a field up to 0.5 T. On the other hand, magnetic domains imaged in 0.5 and 1 T FC experiments show a similar pattern, suggesting saturation of the magnetization reversal process as well as a clear phase separation between ferrimagnetic clusters and the paramagnetic matrix (data taken at 3 T, not shown, are similar to those at 1 T). The lack of correlation between the images
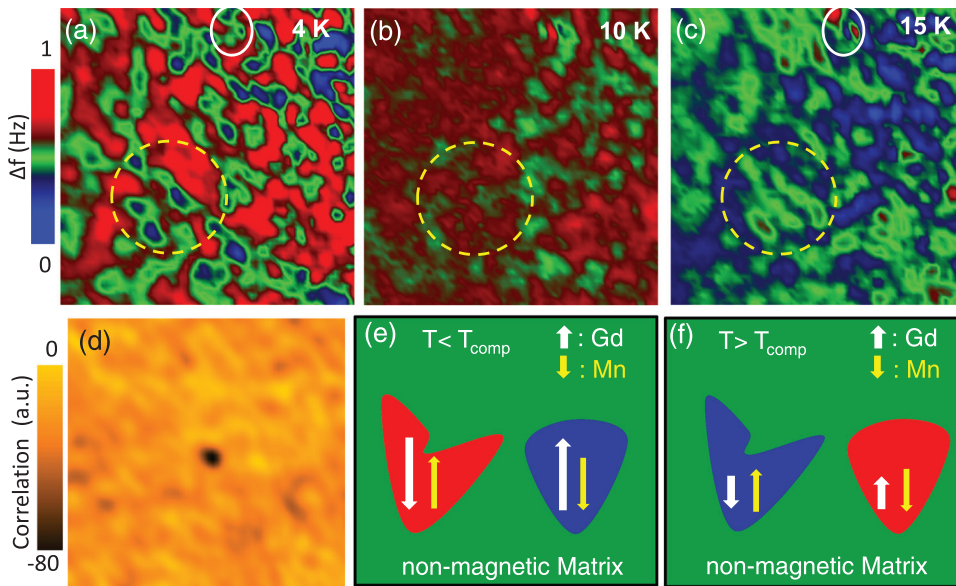
FIG. 2. (Color online) (a)-(c) MFM images acquired at different temperatures. Solid and dashed circles represent the same sample area. (d) Cross-correlation map between images shown in panels (a) and (c). The large negative value at the center of the map signifies the anticorrelation between images. (e), (f) Schematical illustration of the temperature evolution of phase-separated magnetic regions above and below $T_{comp} \approx 12\,K$ in 1 mT. The field of view in the images ((a)-(d)) is $6\,\mu m \times 6\,\mu m$. Features on the left side are broader than those on the right side because the scan plane is not perfectly parallel to the sample surface.
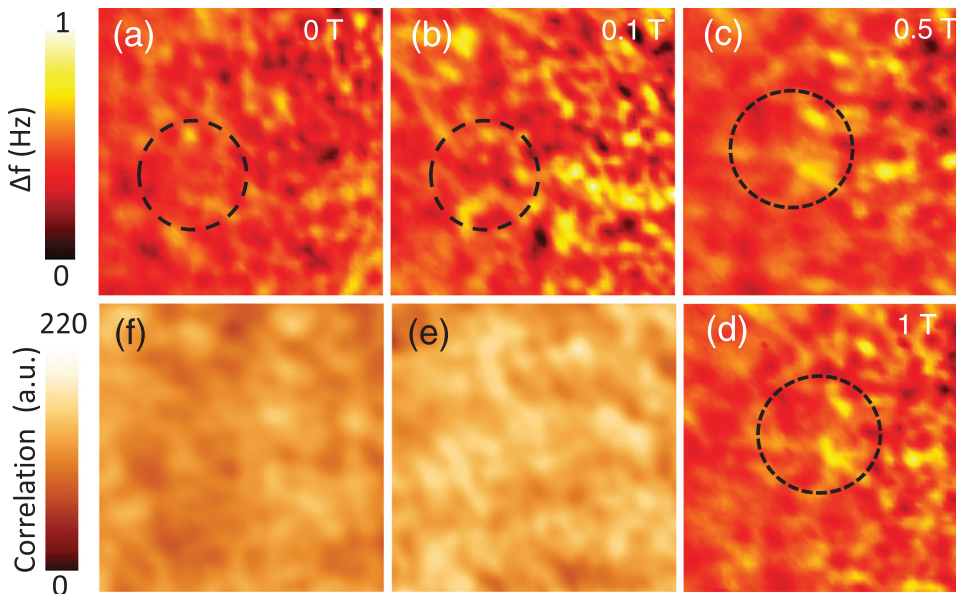

FIG. 3. (Color online) (a)-(d) Field-cooled MFM images taken at 4 K in different magnetic fields. (e), (f) Cross-correlation maps between (a) and (b), and (b) and (c), respectively; no correlation is observed. The field of view in the images ((a)-(f)) is $6\,\mu m \times 6\,\mu m$. Dashed circles correspond to the same sample area.

(a) and (c) cannot be the result of thermal drift of the tip position over the sample, as this was observed repeatedly to be under 1 μm for our system (e.g., see panels (c) and (d)). The magnetic-nonmagnetic phase coexistence could be attributed to localized disorder or a localized strain distribution, similar to observations in Y- and Pr-based manganites with a comparably low tolerance factor [$Y_{2/3}Ca_{1/3}MnO_3$ ($t \sim 0.884$) and $Pr_{2/3}Ca_{1/3}MnO_3$ ($t \sim 0.91$)].[19–22] Results of x-ray diffraction measurements on our thin-film sample, however, are close to those on bulk samples and tend to rule out a strain mechanism of phase separation.

In conclusion, we have performed MFM experiments on a ferrimagnetic GCMO thin film and directly observed phase separation in the sample, with magnetic (FIM) regions of characteristic dimensions between 0.1 and 0.5 μm embedded in a non-magnetic matrix. The behavior of magnetic regions is consistent with the presence of anti-aligned Mn and Gd magnetic sublattices, forming a FIM state. The observed magnetization reversal in the FIM domains as a function of temperature, for small external magnetic field, is consistent with the Mn sublattice being dominant at $T > T_{comp} \approx 15\,K$, but the Gd sublattice (with magnetization locked to be antiparallel to a small applied field) is dominant for $T < T_{comp}$. We attribute the phase separation to localized disorder rather than a strained state of the sample. These results will have significant bearing on the potential utilization of GCMO and other related compounds in magnetic memory device applications.

[1]S. Jin, T. H. Tiefel, M. McCormack, R. A. Fastnacht, R. Ramesh, and L. H. Chen, Science **264**, 413 (1994).

[2]P. A. Lee, N. Nagaosa, and X.-G. Wen, Rev. Mod. Phys. **77**, 721 (2005).

[3]W. Wu, C. Israel, N. Hur, S. Park, S.-W. Cheong, and A. De Lozanne, Nat. Mater. **5**, 881 (2006).

[4]J. P. Zhou, J. T. McDevitt, J. S. Zhou, H. Q. Yin, J. B. Goodenough, Y. Gim, and Q. X. Jia, Appl. Phys. Lett. **75** 1146 (1999).

[5]L. P. Gor'kov and V. Z. Kresinc, Phys. Rep. **400**, 149 (2004).

[6]E. Dagotto, T. Hotta, and A. Moreo, Phys. Rep. **344**, 1 (2001) and references therein.

[7]L. Zhang, C. Israel, A. Biswas, R. L. Greene, and A. de Lozanne, Science **298**, 805 (2002).

[8]J. B. Goodenough, J. Appl. Phys. **81**, 5330 (1997).

[9]H. Y. Hwang, S.-W. Cheong, P. G. Radaelli, M. Marezio, and B. Batlogg, Phys. Rev. Lett. **75**, 914 (1995).

[10]G. J. Snyder, C. H. Booth, F. Bridges, R. Hiskes, S. DiCarolis, M. R. Beasley, and T. H. Geballe, Phys. Rev. B **55**, 6453 (1997).

[11]O. Peña, M. Bahouta, K. Ghanimia, P. Duranb, D. Gutierrezb, and C. Moureb, J. Mater. Chem. **12**, 2480 (2002).

[12]V. F. Correa, N. Haberkorn, G. Nieva, D. J. Garcia, and B. Alascio, e-print arXiv:1109.0259v1.

[13]N. Haberkorn, S. Larrégola, D. Franco, and G. Nieva, J. Magn. Magn. Mater. **321**, 1133 (2009).

[14]Y. Ma, M. Guilloux-Viry, P. Barahona, O. Peña, and C. Moure, Appl. Phys. Lett. **86**, 062506 (2005).

[15]E. Nazaretski, K. S. Graham, J. D. Thompson, J. A. Wright, D. V. Pelekhov, P. C. Hammel, and R. Movshovich, Rev. Sci. Instrum. **80**, 083074 (2009).

[16]A SSS-QMFMR cantilever, Nanosensors, Inc.

[17]Y. H. Sun, Y. G. Zhao, H. F. Tian, C. M. Xiong, B. T. Xie, M. H. Zhu, S. Park, W. Wu, J. Q. Li, and Qi Li, Phys. Rev. B **78**, 024412 (2008).

[18]B. D. Cullity and C. D. Graham, *Introduction to Magnetic Materials* (IEEE Inc., Hoboken, NJ, 2009).

[19]R. Mathieu, P. Nordblad, D. N. H. Nam, N. X. Phuc, and N. V. Khiem, Phys. Rev. B **63**, 174405 (2001).

[20]P. G. Radaelli, R. M. Ibberson, D. N. Argyriou, H. Casalta, K. H. Andersen, S. W. Cheong, and J. F. Mitchell, Phys. Rev. B **63**, 172419 (2001).

[21]V. N. Smolyaninova, A. Biswas, P. Fournier, S. Lofland, X. Zhang, G. Zhao, and R. L. Greene, Phys. Rev. B **65**, 104419 (2002).

[22]D. Saurel, A. Brûlet, A. Heinemann, C. Martin, S. Mercone, and C. Simon, Phys. Rev. B **73**, 094438 (2006).